# Low-Complexity Signal Detection for GSM Based on Group Detection

Xinhe Zhang, Siyu Zhang

*Abstract*—**In order to mitigate the computational complexity of the GSM system, a low-complexity sub-optimal detection algorithm based on group detection and Minimum Mean Square Error (MMSE) detection was proposed in this paper. Firstly, the antenna combinations after group selection were rearranged based on the sorting results of each group of antenna sequences obtained through the sorting algorithm. Subsequently, the MMSE equalization processing detection was applied to the sorted antenna combinations. Then, the modulation symbols obtained after processing were further optimized by combining them with the partial ML algorithm. Finally, the optimal transmit antenna combination and symbols were estimated using the ML algorithm. The simulation results show that the BER performance of the proposed algorithm is comparable to that of the ML algorithm, especially in M-PSK symbol modulation. The BER simulation curve is closer to that of the ML algorithm, while the algorithm's computational complexity is much lower than that of the ML detection algorithm.**

*Index Terms*—**Generalized spatial modulation (GSM), group detection, transmit antenna combination (TAC), bit error rate (BER), computational complexity.**

## I. Introduction

With the rapid development of wireless communication technology, a new type of Multiple-Input Multiple-Output (MIMO) technology, Spatial Modulation (SM), has been proposed [1]-[4]. In an SM system, only one transmit antenna is activated in each time slot, and the antenna itself carries extra information in addition to the transmitted symbol information. This can effectively overcome the issues of Inter-Channel Interference (ICI), Inter-Antenna Synchronization (IAS), and multiple RF links in traditional MIMO systems. Thus, the introduction of SM technology cleverly combines encoding, modulation, and multi-antenna transmission to achieve high spectral efficiency and low complexity wireless transmission. SM technology has been widely recognized as an effective solution for next-generation massive MIMO communication [5]-[6].

Although the SM system has many advantages, its spectral efficiency is lower than that of spatial multiplexing. To address this, Generalized Spatial Modulation (GSM) technology has been proposed [7]-[8]. GSM activates more than one antenna to transmit data in each time slot, with modulation symbols mapped to the combinations of activated antennas. When the activated antennas transmit the same symbol simultaneously, spatial diversity is achieved, which can effectively mitigate ICI to a certain extent. If the activated antennas transmit independent symbols, the spectral efficiency is further improved, along with the transmission rate. Therefore, GSM technology overcomes the limitations of traditional SM systems regarding the number of transmit antennas by flexibly selecting the number of transmit antennas and activated antennas in each time slot. By utilizing independent data transmission and spatial multiplexing methods, GSM can achieve the same or even higher spectral efficiency compared to SM systems.

The signal demodulation algorithms at the receiver of the GSM system include the optimal detection algorithm and the sub-optimal detection algorithms. The optimal detection algorithm is the Maximum Likelihood (ML) detection algorithm, as proposed in [9]. Its main idea is to traverse all possible combinations of transmit antenna and symbols. However, as the number of antenna combinations and modulation orders increases, the computational complexity of the algorithm also increases exponentially. To address this issue, various sub-optimal detection algorithms have been proposed in [10]-[20].

A sub-optimal detection algorithm based on the Zero Forcing (ZF) detector is proposed in [10]. This algorithm eliminates mutual interference between signals by applying pseudo-inverse matrix operations to separate and demodulate signals. The Ordered Block Minimum Mean Square Error (OB-MMSE) detection algorithm, proposed in [11], sorts all antenna combinations using pseudo-inverse operations to calculate weights, and then employs the MMSE criterion to achieve the optimal signal estimation. This approach offers advantages in suppressing multipath fading and resisting noise interference. A novel grouping idea has been proposed in [12]-[13]. The Group Maximum Likelihood (GML) detection algorithm presented in [12] takes into account the mapping table of transmit antenna combinations and applies the ML detector to the established groups, achieving optimal partitioning to the vectors to be detected. This results in good performance and ultra-low complexity for the system under a fixed wireless channel. [13] introduces a Nested Maximum Likelihood Group (NMLG) detection algorithm, which continuously utilizes the ML detector in a nested manner for equalized received signals and offers significant performance advantages. Additionally, [14] introduces a low-complexity detection algorithm implemented in a grouped manner. This algorithm groups the transmit antenna based on the number of activated antennas and performs corresponding group

Manuscript received July 19, 2024; revised March 3, 2025.

This work was supported in part by the scientific Research Fund of Liaoning Provincial Education Department of China under Grant LJKZ0292.

Xinhe Zhang is an associate professor of School of Electronic and Information Engineering, University of Science and Technology Liaoning, Anshan, 114051 China. (corresponding author phone: 86-412-5929738; email: 527075114@qq.com).

Siyu Zhang is a postgraduate of School of Electronic and Information Engineering, University of Science and Technology Liaoning, Anshan, 114051 China. (e-mail: 463720154@qq.com).

serial detection at the receiver. Simulations demonstrates the algorithm's good performance.

[15] proposed a Projection-Based List Detection (PBLD) algorithm, which generates a series of candidate transmission signals through multi-step detection. These candidates are then sorted based on the proximity of their data vectors to one of the possible subsets of vectors. The algorithm employs a quality metric to select the best candidate items and a list length metric to manage the size of the list. In [16], a Fully-Generalized Spatial Modulation (F-GSM) system is described. This system is characterized by an increase in data transmission rate as the number of transmit antennas increases, providing a faster data transmission rate compared to the previous GSM systems.

To approximate the bit error rate (BER) performance of the ML detection algorithm while significantly reducing computational complexity, we propose a sub-optimal low-complexity detection algorithm for GSM systems transmitting independent signals — the Group Partial Maximum Likelihood detection algorithm based on Minimum Mean Square Error (GP-MMSE). In this group detection algorithm, 'grouping' refers to the optimal division of all known transmit antennas into groups, with each group containing the same number of antennas. Subsequently, a specific number of antennas within each group are activated for data transmission, effectively reducing system complexity. For demodulating symbols in SM systems, two detection algorithms are introduced: the HL-ML and LC-ML detection algorithms. Their modulation process is independent of the modulation order M [17] - [18]. The main contributions of this paper are as follows.

1) To reduce the computational complexity of ML detector in GSM systems, an improved grouping strategy is employed to narrow down the search range of potential antenna combinations.

2) To achieve optimal detection performance, we employ the group partial ML detection algorithm combined with the MMSE algorithm to estimate the transmit antenna combination. Additionally, we utilize the hard-limited ML algorithm to estimate the modulation symbols.

The remainder of this paper is organized as follows. Section II presents the system model of GSM. Section III introduces an improved low complexity sub-optimal detection algorithm. Section IV provides experimental simulation analysis, including the calculation and analysis of the computational complexity of the corresponding algorithm. Finally, Section V concludes the paper.

Notation: $(\cdot)^{-1}$, $(\cdot)^{\mathrm{T}}$, $(\cdot)^{\mathrm{H}}$ and $(\cdot)^{\dagger}$ represent the inverse, transpose, conjugate transpose and pseudo-inverse of a vector or a matrix, respectively. $\lfloor\cdot\rfloor$ denotes the floor operation, which rounds a real number down to the nearest integer. $\|\cdot\|_F$ is the Frobenius norm of a vector or a matrix. $\|\cdot\|_2$ represents the $\ell_2$-norm of a matrix or a vector. $|\cdot|$ stands for the absolute value of a real or complex number, or the cardinality of a given set. $\Re(\cdot)$ and $\Im(\cdot)$ are the real and imaginary parts of a complex-valued variable, respectively. $round(\cdot)$ indicates the operation of rounding a real number to the nearest integer. $\mathrm{mod}(\cdot,\cdot)$ is the modulo operation. $\min(\cdot)$ and $\max(\cdot)$ represent the minimum and maximum values, respectively. $C_n^k = \frac{n!}{k!(n-k)!}$ denotes the binomial coefficient, which represents the number of ways to choose $k$ elements from a set of $n$ elements. $\mathbb{C}$ represents the field of complex numbers.

## II. System model

Assuming a GSM system has $N_t$ transmit antenna and $N_r$ receive antennas, and only $N_p$ transmit antennas are activated in each time slot, each of which simultaneously transmits modulation symbols. The modulation mode employed is M-QAM or M-PSK constellation modulation. Therefore, there are a total of $N = C_{N_t}^{N_p}$ possible combinations of transmit antennas. However, according to the mapping principle of the GSM system, the number of available antenna combinations must be an integer power of 2. So, the actual number of effective activated antenna combinations is $N_c = 2^{\left\lfloor \log_2 C_{N_t}^{N_p} \right\rfloor}$. The GSM system splits the binary information bit stream into two parts: one part is used to specify the transmit antenna combination for the ongoing data transmission, and the other part is used to choose the modulation symbol. When $N_c$ activated antenna combinations transmit independent modulation symbol vectors $\boldsymbol{s} = [s_1, s_2, \cdots s_{N_p}]^T$, $s_1, s_2, \cdots, s_{N_p} \in S$, the length of the information bit sequence for specifying the activated antenna combination is $R_1 = \left\lfloor \log_2 C_{N_t}^{N_p} \right\rfloor$, and the length of the information bit sequence for choosing the modulation symbol is $R_2 = N_p \log_2 M$, where $M$ represents modulation order, $S$ denotes the set of modulation symbols. The length of the information bits transmitted by the GSM system per time slot can be expressed as follows.

$$R_{\mathrm{GSM}} = \left\lfloor \log_2 C_{N_t}^{N_p} \right\rfloor + N_p \log_2 M \tag{1}$$

The modulation symbol vector $\boldsymbol{s}$ is transmitted through the channel gain matrix $\boldsymbol{H} \in \mathbb{C}^{N_t \times N_r}$, and the system model of the received signal $\boldsymbol{y}$ can be represented as follows.

$$\boldsymbol{y} = \boldsymbol{H}\boldsymbol{x} + \boldsymbol{n} \tag{2}$$

Where $\boldsymbol{H}$ follows a complex Gaussian distribution with a mean of 0 and a variance of 1, each element $h_{i,j}$ represents the channel gain between the $i$-th transmit antenna and the $j$-th receive antenna. $\boldsymbol{x} \in \mathbb{C}^{N_t \times 1}$ represents the transmit signal vector, $\boldsymbol{y} \in \mathbb{C}^{N_r \times 1}$ represents the received signal vector, and $\boldsymbol{n} \in \mathbb{C}^{N_r \times 1}$ represents the additive noise vector. each element of $\boldsymbol{n}$ is independent of each other and follows a complex Gaussian distribution with a mean of 0 and a variance of $\sigma^2$. The transmit signal vector $\boldsymbol{x}$ can be represented as:

$$\boldsymbol{x} = [0, \cdots, 0, s_1, 0, \cdots, 0, s_2, 0 \cdots, 0, s_{N_p}, 0, \cdots]^T \tag{3}$$

In Eq. (3), the non-zero elements represent independent transmit symbols, each originating from different activated antennas. The positions of these non-zero elements within the vector correspond the indices of the active antennas. The total number of these non-zeros elements is equal to the number of activated antennas, denoted as $N_p$.

Assuming that the $I$-th antenna combination in the current time slot is used to transmit modulation symbols, the received signal vector $\boldsymbol{y}$ in Eq. (2) can be considered equivalent to

$$\boldsymbol{y} = \sum_{l=i_1}^{i_{N_p}} \boldsymbol{h}_l \boldsymbol{s}_l + \boldsymbol{n} = \boldsymbol{H}_I \boldsymbol{s} + \boldsymbol{n} \tag{4}$$

$i_1, i_2, \cdots, i_{N_p}$ represent the indices of $N_p$ activated antennas in the antenna combination with sequence $I$, $l$ is the index of one of the activated antennas, $I \in \{1, 2, \cdots, N_c\}$. $\boldsymbol{h}_l$ is the $l$-th column of the channel gain matrix $\boldsymbol{H}$, and $\boldsymbol{H}_I = \left(h_{i_1}, h_{i_2}, \cdots, h_{i_{N_p}}\right) \in \mathbb{C}^{N_r \times N_p}$ is a submatrix of the channel matrix $\boldsymbol{H}$ corresponding to the current $I$-th transmit antenna combination.

In the GSM system, the ML detection algorithm exhaustively searches for all possible combinations of transmit antennas and their corresponding modulation symbols. It compares the Euclidean distance between each possible combination and the received signal vector $\boldsymbol{y}$, and performs joint detection across all sets of transmit antenna combinations and modulation symbols. The vector that corresponds to the minimum Euclidean distance is considered the final detection result. The ML detector can be mathematically represented as follows:

$$\left(\hat{I}, \hat{\boldsymbol{s}}\right) = \arg \min_{I \in Q, s \in S} \| \boldsymbol{y} - \boldsymbol{H}_I \boldsymbol{s} \|_2^2 \tag{5}$$

where $\hat{I} \in I$ denotes the final estimated activated antenna combination in the current time slot, $I \in Q = \left\{I_1, I_2, \cdots, I_{N_c}\right\}$ denotes the set of possible activated antenna combinations, $\hat{\boldsymbol{s}}$ denotes the modulation symbols transmitted by the activated antennas, and $\boldsymbol{H}_I$ denotes the sub-matrix of the channel matrix $\boldsymbol{H}$ corresponding to the $\hat{I}$-th activated antenna combination.

From Eq. (5), it can be observed that for GSM systems transmitting independent signals, the ML algorithm requires performing $N_c M^{N_p}$ traversal search. Although the ML algorithm exhibits the optimal BER performance and the highest accuracy in estimating the transmit antenna combination and modulation symbols, its computational complexity is extremely high, making it challenging to implement in large-scale antenna GSM systems.

## III. GP-MMSE Detection Algorithm

The group detection technique is inspired by the GML detection algorithm [12]. To enhance the performance of GSM systems, this section incorporates the grouping idea from the GML algorithm into GSM systems and further increases the grouping size. Additionally, a low-complexity GP-MMSE detection algorithm is proposed, which combines the MMSE equalized processing detection algorithm with the partial ML detection algorithm.

First, the $N_t$ transmit antennas are divided into $N_p$ groups, with only one antenna activated in each group. The pseudo-inverse of each column of the channel matrix is used to preprocess the received signals, and to sort the indices of the transmit antennas within each group. Subsequently, all possible transmit antenna combinations are reordered based on the sorted indices of antennas within each group. Next, these sorted combinations are sequentially demodulated using the MMSE equalization processor for symbol demodulation. A judgment threshold is then introduced to further narrow down the search range. If no judgment condition is met, the ML detection is ultimately employed to obtain the minimum Euclidean distance, thereby estimating the required activated antenna combination and transmit symbols. Finally, the set of adjacent constellation points that minimizes the estimated symbol constellation distance is identified. Subsequently, the partial ML algorithm is applied for demodulation and re-detection, enhancing the accuracy of the symbol decision result [21]. The specific steps of this algorithm are as follows.

Step 1: In a GSM system with $N_t$ transmit antennas, we activate $N_p$ transmit antennas for transmitting modulation symbols in each time slot. All antennas can be divided into $N_p$ groups, each consisting of $N = N_t / N_p$ antennas. When information is transmitted, only one antenna from each group can be selected for transmission. Therefore, there are a total of $(N_t/N_p)^{N_p}$ types of transmit antenna combinations. However, since the number of available antenna combinations can only be a power of 2, the effective number of antenna combinations is $N_c = 2^{\lfloor N_p \log_2(N_t/N_p) \rfloor}$. Figure 1 illustrates the grouping rules of the transmit antenna for the scenario of $N_t = 6, N_p = 3$.

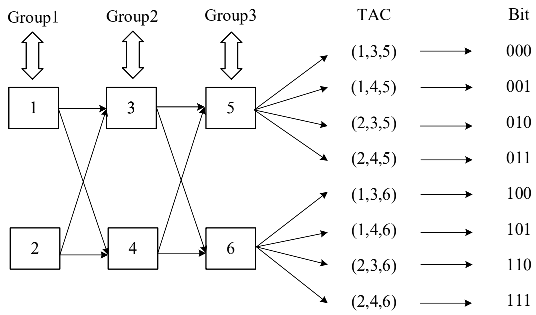


Fig. 1. Grouping rules of the transmit antennas for $N_t = 6, N_p = 3$.

Step 2: Process the received signal vector $\boldsymbol{y}$ using the pseudo-inverse of each column of the channel matrix $\boldsymbol{H}$ to measure the activation possibility of all transmit antennas, resulting in $\boldsymbol{z} = \left[z_1, z_2, \cdots, z_{N_t}\right]^{\mathrm{T}}$, where $z_k$ is represented as:

$$z_k = \left\|(\boldsymbol{h}_k)^{\dagger} \boldsymbol{y}\right\|_2 = \left\|\frac{\boldsymbol{h}_k^{\mathrm{H}} \boldsymbol{y}}{\boldsymbol{h}_k^{\mathrm{H}} \boldsymbol{h}_k}\right\|_2 \tag{6}$$

where $\boldsymbol{h}_k$ represents the $k$-th column of the channel matrix $\boldsymbol{H}$, $(\boldsymbol{h}_k)^{\dagger} = \dfrac{\boldsymbol{h}_k^{\mathrm{H}}}{\boldsymbol{h}_k^{\mathrm{H}} \boldsymbol{h}_k}$ represents the pseudo-inverse operation on the vector of channel matrix $\boldsymbol{H}$, $k \in \{1, 2, \cdots, N_t/N_p\}$.

Step 3: Sort the transmit antennas within each group based on their corresponding $z$ value. The sorted groups are illustrated in Figure 1. In this example, there are three groups of transmit antennas, with each group containing two transmit antennas. Within each group, the antennas are arranged in ascending order according to their $z$ values. In the first set, there are:

$$\left[k_1, k_2\right] = \arg sort\left(\boldsymbol{z}_1\right) \tag{7}$$

In group 1, the antennas are ordered based on their activation possibility, with $k_1$ and $k_2$ denoting the indices of the antennas in this order. Specially, $k_1$ represents the index of the antenna with the highest possibility of activation with the group, and $k_2$ represents the index of the antenna with the second highest possibility of activation. $\boldsymbol{z}_1 = \left[z_1, z_2\right]^T$ is the submatrix of vector $\boldsymbol{z}$. Correspondingly, the sort results for the antennas in the other two groups are given by Eqs. (8) and (9), respectively:

$$\left[k_3, k_4\right] = \arg sort\left(\boldsymbol{z}_2\right) \tag{8}$$

$$\left[k_5, k_6\right] = \arg sort\left(\boldsymbol{z}_3\right) \tag{9}$$

where $\boldsymbol{z}_2 = \left[z_3, z_4\right]^{\mathrm{T}}, \boldsymbol{z}_3 = \left[z_5, z_6\right]^{\mathrm{T}}$.

Next, we generalized this example to a general case. Assuming that in a GSM system, there are $N_t$ transmit antennas and $N_p$ activated antennas, the sub-matrixes of vector $\boldsymbol{z}$ are as follows.

$$\begin{cases} \boldsymbol{z}_1 = \left[ z_1, z_2, \cdots, z_{\frac{N_t}{N_p}} \right]^{\mathrm{T}} \\ \boldsymbol{z}_2 = \left[ z_{\frac{N_t}{N_p}+1}, z_{\frac{N_t}{N_p}+2}, \cdots, z_{\frac{2N_t}{N_p}} \right]^{\mathrm{T}} \\ \cdots \\ \boldsymbol{z}_{N_p} = \left[ z_{(N_p-1)\frac{N_t}{N_p}+1}, z_{(N_p-1)\frac{N_t}{N_p}+2}, \cdots, z_{N_t} \right]^{\mathrm{T}} \end{cases} \tag{10}$$

The sort result of each antenna set is as follows:

$$\begin{cases} \left[ k_1, k_2, \cdots, k_{\frac{N_t}{N_p}} \right] = \arg sort(\boldsymbol{z}_1) \\ \left[ k_{\frac{N_t}{N_p}+1}, k_{\frac{N_t}{N_p}+2}, \cdots, k_{\frac{2N_t}{N_p}} \right] = \arg sort(\boldsymbol{z}_2) \\ \cdots \\ \left[ k_{\frac{(N_p-1)N_t}{N_p}+1}, k_{\frac{(N_p-1)N_t}{N_p}+2}, \cdots, k_{N_t} \right] = \arg sort(\boldsymbol{z}_{N_p}) \end{cases} \tag{11}$$

where $k_1, k_{\frac{N_t}{N_p}+1}, \cdots, k_{\frac{(N_p-1)N_t}{N_p}+1}$ are the indices of the antennas with the highest activation probability in each group.

Step 4: Reorder all activated antenna combinations according to the sorting results of each group of transmitting antennas in Step 3. Firstly, determine the order of the first activated antenna in the first antenna set. Then, reorder the antenna combinations containing $k_1, k_2, \cdots, k_{N_t/N_p}$ antenna indices according to the order determined in Step 3. Assuming that the sorting result of group 1's $\left[k_1, k_2\right]$ in Figure 1 is [2,1], the sorting result of the antenna combination is shown in Figure 2.

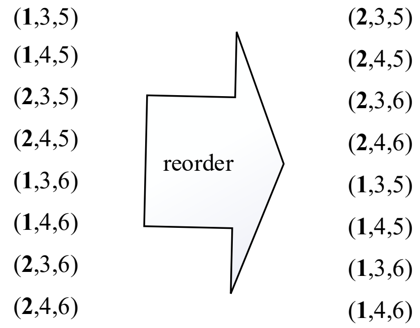


Fig. 2. The first step sorting rules of the transmit antennas for $N_t = 6, N_p = 3$.

Step 5: Without affecting the order of the first activated antenna, we rearrange the second activated antenna in the order of index $k_{\frac{N_t}{N_p}+1}, k_{\frac{N_t}{N_p}+2}, \cdots, k_{\frac{2N_t}{N_p}}$ in the second antenna set. If the sorting result of $\left[k_3, k_4\right]$ in group 2 is [4,3], we should first prioritize the transmit antenna combinations that include antenna index 4, and then proceed to rank the combinations that include index 3. The sorting rule is illustrated in Figure 3.

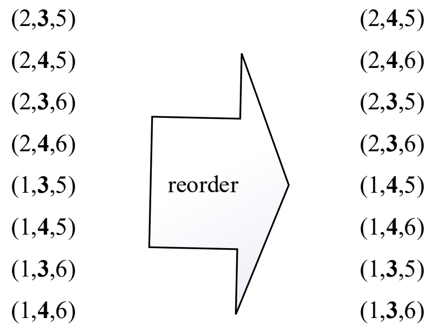


Fig. 3. The second step sorting rules of the transmit antennas for $N_t = 6, N_p = 3$.

Step 6: According to the above sorting rules, the antenna indices in group 3, as well as those in group $N_p$, are further sorted until all $N_t$ transmit antennas have been properly sorted.

When this sorting rule is generalized to the general case, there are $N_p$ activated antennas, and all $N_t$ transmit antennas are divided into $N_p$ groups. In the specific case where only one antenna is activated in each group, there are $\left(N_t / N_p\right)^{N_p}$ possible combinations. The transmit antenna indices will be sorted as shown in Figure 4, where the combinations of activated transmit antennas are arranged from left to right.

As shown in Figure 4, the antenna combination $\left( k_1, k_{\frac{N_t}{N_p}+1}, \cdots, k_{\frac{(N_p-1)N_t}{N_p}+1} \right)$ located at the leftmost position is the most likely one to be activated.

Step 7: Sequentially perform the block MMSE equalization processing on each of the reordered transmit antenna combinations, as defined in Eq. (12):

$$\tilde{\boldsymbol{s}}_j=\left(\left(\boldsymbol{H}_{I_{k_j}}\right)^{\mathrm{H}}\boldsymbol{H}_{I_{k_j}}+\sigma^2\boldsymbol{I}\right)^{-1}\left(\boldsymbol{H}_{I_{k_j}}\right)^{\mathrm{H}}\boldsymbol{y} \tag{12}$$

where $\tilde{\boldsymbol{s}}_j$ is the detected symbol in the $j$-th antenna combination in the new ordered set, $\boldsymbol{I}$ is the $N_p \times N_p$ identity matrix, and $\boldsymbol{H}_{I_{k_j}} \in \mathbb{C}^{N_r \times N_p}$ consists of the column vectors of all antenna indices corresponding to the $j$-th antenna combination $I_{k_j}$ in the channel matrix $\boldsymbol{H}$ after ordering.

Step 8: Symbol demodulation for M-QAM and M-PSK constellations is performed for the symbol $\tilde{\boldsymbol{s}}_j$ obtained in $j$-th antenna combination $I_{k_j}$, respectively.

For the M-QAM constellation, if the modulation signal $S$, with $|S|=M$, forms a square or rectangular lattice constellation, then the constellation can be regarded as the Cartesian product of two sets $S_1 = N_1$-PAM and $S_2 = N_2$-PAM, where the values of $N_1$ and $N_2$ are given by $N\text{-PAM}=\{-N+1,-N+3,\cdots,-1,1,\cdots,N-3,N-1\}$. $N$ is the positive integer powers of 2. The real and imaginary parts of the modulation symbol $\tilde{s}_j$ are quantized separately, as illustrated in Eqs. (13)-(14). Subsequently, these quantized real and imaginary parts are recombined using Eq. (15) to achieve M-QAM constellation modulation.

$$\Re\left(\boldsymbol{s}_j\right)=\min\left[\max\left(2*round\left[\frac{\Re\left(\tilde{\boldsymbol{s}}_j\right)+1}{2}\right]-1,-N_1+1\right),N_1-1\right] \tag{13}$$

$$\Im\left(\boldsymbol{s}_j\right)=\min\left[\max\left(2*round\left[\frac{\Im\left(\tilde{\boldsymbol{s}}_j\right)+1}{2}\right]-1,-N_2+1\right),N_2-1\right] \tag{14}$$

$$\boldsymbol{s}_j=\Re\left(\boldsymbol{s}_j\right)+j\Im\left(\boldsymbol{s}_j\right) \tag{15}$$

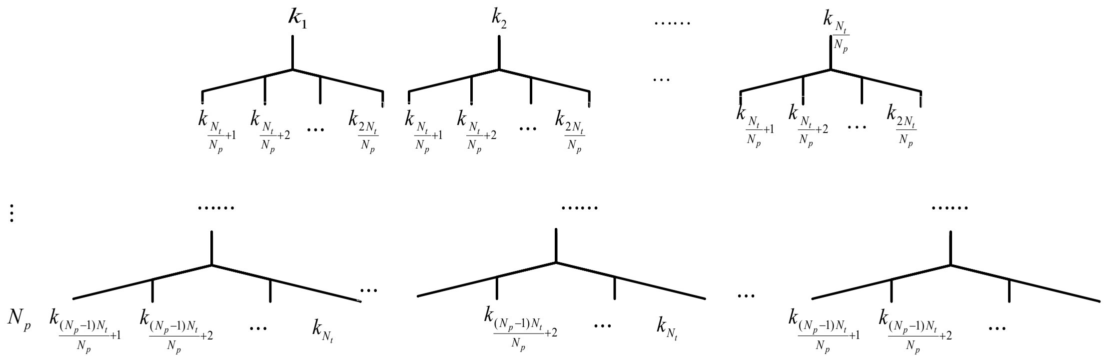


Fig. 4. The sorting rule of antennas in general.

In an M-PSK constellation, the constellation points are located on a unit circle with an amplitude of 1, each representing a unique phase. The quantization of the modulation symbol $\tilde{\boldsymbol{s}}_j$ is different from that of the M-QAM constellation. Assuming $\theta$ is the angle between $\tilde{\boldsymbol{s}}_j$ and the positive real axis of the complex plane, the quantization symbol $\boldsymbol{s}_j$ after the $j$-th antenna combination correction can be represented by Eqs. (16)-(18).

$$\varphi_j=\frac{\theta M}{2\pi} \tag{16}$$

$$\hat{\varphi}_j=\mathrm{mod}\left(round\left(\varphi_j\right),M\right)*\frac{2\pi}{M} \tag{17}$$

$$\boldsymbol{s}_j=\cos\hat{\varphi}_j+j\sin\hat{\varphi}_j \tag{18}$$

Step 9: After quantizing the modulation symbols $\tilde{\boldsymbol{s}}_j$, a judgment threshold is introduced to constrain the possible conditions of the both transmit antenna combinations $I_{k_j}$ and the transmit symbols $\boldsymbol{s}_j$, with the aim of reducing the computational complexity,. If the condition specified by Eq. (19) is satisfied, the output is $(I_{k_j},\boldsymbol{s}_j)$.

$$d_j=\left\|\boldsymbol{y}-\boldsymbol{H}_{I_{k_j}}\boldsymbol{s}_j\right\|_2^2\le \mathrm{V_{th}} \tag{19}$$

where $\mathrm{V_{th}}$ is a preset threshold for judging whether the detected signal meets the condition. The judgment threshold $\mathrm{V_{th}}$ is set to $2N_r\sigma^2$. If the current detected result satisfies the condition given by Eq. (19), it is considered that the detector has successfully found the optimal estimates $\hat{I}$ and $\hat{\boldsymbol{s}}$. If $d_j > \mathrm{V_{th}}$ is obtained for the current detection, it is deemed that group $(I_{k_j},\boldsymbol{s}_j)$ is not the optimal estimation result. Hence, the detector updates $j=j+1$ and proceeds to detect whether the next group satisfies the condition.

Step 10: If no candidate $(I_{k_j},\boldsymbol{s}_j)$ meets the condition given by Eq. (19), the optimal result is estimated using the ML detection algorithm.

$$\begin{cases}\hat{j}=\arg\min\limits_j\left\|\boldsymbol{y}-\boldsymbol{H}_{I_{k_j}}\boldsymbol{s}_j\right\|_2^2=\arg\min\limits_j\boldsymbol{d}\ ,\ j\in\{1,2,\cdots,N_c\}\\ \hat{I}=I_{\hat{j}}\ ,\ \ \hat{\boldsymbol{s}}=\boldsymbol{s}_{\hat{j}}\end{cases} \tag{20}$$

where $\left\|\boldsymbol{y}-\boldsymbol{H}_{I_{k_j}}\boldsymbol{s}_j\right\|_2^2$ in ML detection is the set of $d_j$, which is denoted as matrix $\boldsymbol{d}\in\mathbb{C}^{1\times N_c}$. Then, the currently detected $(\hat{I},\hat{\boldsymbol{s}})$ is deemed as the optimal estimate.

Step 11: The obtained modulated symbols $\boldsymbol{s}_j$ are re-detected using partial ML. The set of adjacent constellation points with the smallest Euclidean distance to the detected symbol $\boldsymbol{s}_{\hat{j}}$, specifically those whose Hamming distance is 1, is identified. Figures 5-6 illustrate the sets of constellation points closest to $\boldsymbol{s}_{\hat{j}}$ using 16QAM and 8PSK modulation, respectively.

As illustrated in Figure 5, in 16-QAM modulation, adjacent constellation points can differ by values of 2, 3, or 4. For instance, if the modulation symbol $\boldsymbol{s}_{\hat{j}}$ is 1101, then its adjacent constellation points are 0101, 1100, 1001, and 1111. However, in Figure 6, only two adjacent constellation points are present for each constellation symbol in M-PSK modulation.

Step 12: The ML detection algorithm is once again applied to the set of constellation points, with the aim of correcting the modulation symbol $\boldsymbol{s}_{\hat{j}}$. The constellation point $\boldsymbol{s}_{\hat{j}}$ with the minimum Euclidean distance from the receiver vector $\boldsymbol{y}$ is selected as the output, as shown in Eq. (21).

$$\begin{cases} \hat{j} = \arg\min\limits_{j} \left\| \boldsymbol{y} - \widehat{\boldsymbol{H}}_{\hat{I}} \widehat{\boldsymbol{s}}_{j} \right\|_2^2 \\ \hat{\boldsymbol{s}} = \boldsymbol{s}_{\hat{j}} \end{cases} \tag{21}$$

where $\widehat{\boldsymbol{H}}_{\hat{I}} \in \mathbb{C}^{N_r \times N_p}$ is composed of column vectors corresponding to the indices of the detected optimal activated antenna combination $\hat{I}$ in channel matrix $\boldsymbol{H}$, and $\widehat{\boldsymbol{s}}_{j}$ represents the set of constellation symbol $\boldsymbol{s}_{\hat{j}}$ and adjacent constellation points with the smallest distance from $\boldsymbol{s}_{\hat{j}}$.

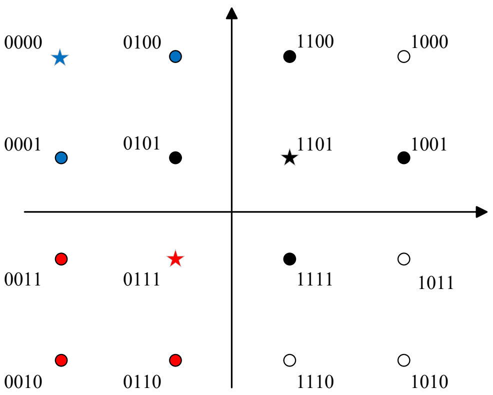


Fig. 5. Adjacent constellation points for 16QAM.

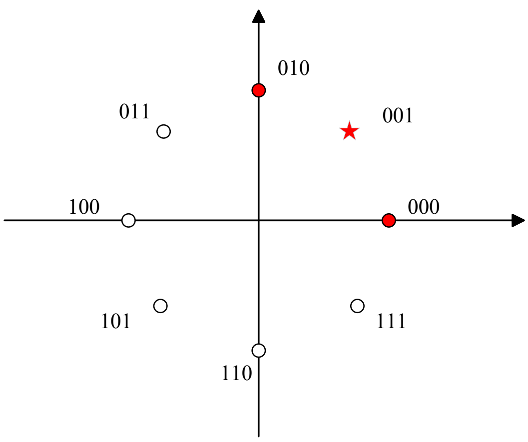


Fig. 6. Adjacent constellation points for 8PSK constellation.

Finally, both the optimal activation antenna combination $\hat{I}$ and the transmit modulation symbols $\boldsymbol{s}_{\hat{j}}$ have been successfully detected. The ML algorithm, by detecting only a subset of the constellation points and avoiding a full search through all possible points, significantly reduces its computational complexity compared to the ML algorithm that employs exhaustive search.

The proposed GP-MMSE detection algorithm can be described in Table I.

TABLE I
PROPOSED GP-MMSE DETECTION ALGORITHM

1: Input: $\boldsymbol{y}$, $\boldsymbol{H}$, $N_t$, $N_r$, $N_p$, $\mathrm{V_{th}} = 2N_r\sigma^2$.

2: Divide the $N_t$ transmit antennas into $N_p$ groups, with each group containing $N_t/N_p$ antennas;

3: Process the received signals $\boldsymbol{y}$ using each column of channel matrix $\boldsymbol{H}$ to obtain vector $z = \left[z_1, z_2, \cdots, z_{N_t}\right]^T$ : $z_k = \left\|(\boldsymbol{h}_k)^{\dagger}\boldsymbol{y}\right\| = \left\|\dfrac{\boldsymbol{h}_k^{\mathrm{H}}\boldsymbol{y}}{\boldsymbol{h}_k^{\mathrm{H}}\boldsymbol{h}_k}\right\|_2^2$ ;

4: Use Eq. (10) to group $z$ into $N_p$ sets, and then sort the transmit antennas within each set according to their corresponding values as determined by Eq. (11);

5: Reorder the transmit antenna combinations in the order of $k_j$, and while maintaining the order of the previous active antenna, further sort the indices in subsequent antenna set until the process is repeated $N_p$ times, resulting in a new ordering of the antenna combinations;

6: **Initialize** $j = 1$ ;

7: **while** $j \le N_c$

8: **do** $\boldsymbol{s}_j = Q\left(\left(\left(\boldsymbol{H}_{I_{k_j}}\right)^{\mathrm{H}} \boldsymbol{H}_{I_{k_j}} + \sigma^2 \boldsymbol{I}\right)^{-1} \left(\boldsymbol{H}_{I_{k_j}}\right)^{\mathrm{H}} \boldsymbol{y}\right)$, $d_j = \left\|\boldsymbol{y} - \boldsymbol{H}_{I_{k_j}} \boldsymbol{s}_j\right\|_2^2$ ;

9: **if** $d_j \le \mathrm{V_{th}}$

$\hat{I} = I_{k_j}, \hat{\boldsymbol{s}} = \boldsymbol{s}_j$ ,**break**;

10: **else**

$j = j + 1$ ;

11: **end if**

12: **end while**

13: **if** $j > N_c$

$$\begin{cases} \hat{j} = \arg\min\limits_{j} \left\|\boldsymbol{y} - \boldsymbol{H}_{I_{k_j}} \boldsymbol{s}_j\right\|_2^2 = \arg\min\limits_{j} \boldsymbol{d} \ , \ j \in \{1, 2, \cdots, N_c\} \\ \hat{I} = I_{\hat{j}} \ , \ \hat{\boldsymbol{s}} = \boldsymbol{s}_{\hat{j}} \end{cases}$$

14: **end if**

15: Identify the constellation symbol $\boldsymbol{s}_{\hat{j}}$ and determine the adjacent constellation point that has the smallest Euclidean distance from $\boldsymbol{s}_{\hat{j}}$ to form the set $\widehat{\boldsymbol{s}}_j$ ;

16: The modulation symbols are corrected using ML:

$$\begin{cases} \hat{j} = \arg\min\limits_{j} \left\|\boldsymbol{y} - \widehat{\boldsymbol{H}}_{\hat{I}} \widehat{\boldsymbol{s}}_j\right\|_2^2 \\ \hat{\boldsymbol{s}} = \boldsymbol{s}_{\hat{j}} \end{cases}$$

17: Output the final result $\left(\hat{I}, \hat{\boldsymbol{s}}\right)$.

## IV. Simulation Results and Computational Complexity Analysis

To verify the BER performance and computational complexity of the proposed GP-MMSE algorithm, as well as the ML and OB-MMSE algorithms, simulations were conducted using both M-QAM modulation and M-PSK modulation schemes. Assuming a GSM system where activated antennas transmit independent signals, the BER performance of these three algorithms was compared at various signal-to-noise ratios (SNRs). The simulations were performed in a quasi-static Rayleigh flat fading channel, with additive Gaussian white noise following a complex Gaussian distribution having a mean of 0 and a variance of 1.

### *A. BER performance with M-QAM modulation*

Figure 7 provides a comparison of the BER performance of ML, OB-MMSE, and GP-MMSE algorithms under 16QAM modulation simulation scenarios in GSM systems with $N_t = 8$, $N_r = 12$, and $N_p = 2$. The horizontal axis represents the SNR, and the vertical axis represents the BER performance. It can be observed that the BER performance of the GP-MMSE algorithm is superior to that of the OB-MMSE algorithm, and its BER performance is closer to the ML algorithm.

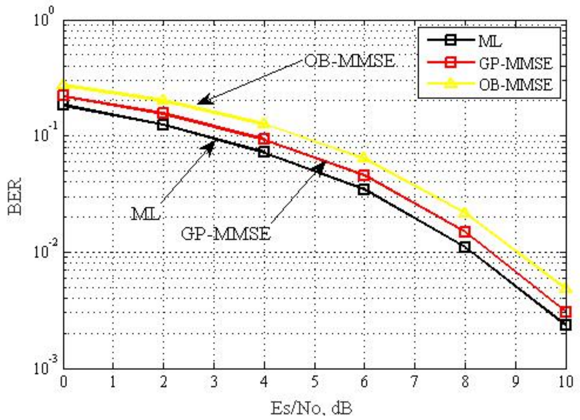


Fig. 7. Comparison of BER performance of ML, OB-MMSE, and GP-MMSE algorithms with $N_t = 8$, $N_r = 12$, $N_p = 2$ for 16QAM constellation.

Figure 8 shows a comparison of the BER performance of ML, OB-MMSE, and GP-MMSE algorithms under the condition of $N_t = 6$, $N_r = 10$, $N_p = 3$, $M = 16$. As shown in Figure 8, the BER performance of the GP-MMSE algorithm is superior to that of the OB-MMSE algorithm, and its BER performance is closer to the ML algorithm.

### *B. BER performance with M-PSK modulation*

Figure 9 provides a comparison of the BER performance of ML, OB-MMSE, and GP-MMSE algorithms under 16PSK modulation simulation scenarios in GSM system with $N_t = 8$, $N_r = 12$, $N_p = 3$. It can be observed that the BER performance of the proposed GP-MMSE algorithm closely approximates the simulation curve of the ML algorithm, demonstrating excellent simulation performance. When the SNR exceeds 10dB, the BER performance of the GP-MMSE algorithm matches that of the ML algorithm. In contrast, the simulation curve of the OB-MMSE algorithm is slightly inferior, with its performance being marginally lower than that of the GP-MMSE algorithm when the SNR is above 6dB.

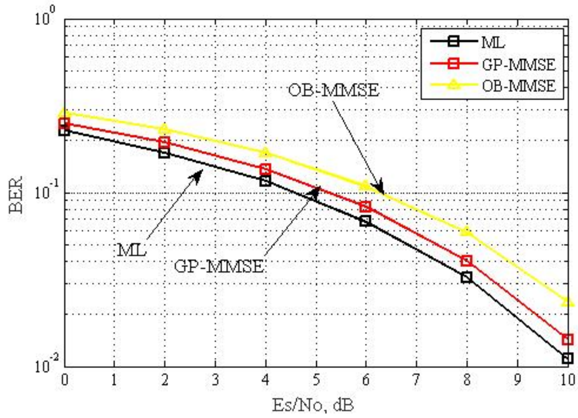


Fig. 8. Comparison of BER performance of ML, OB-MMSE, and GP-MMSE algorithms with $N_t = 6$, $N_r = 10$, $N_p = 3$ for 16QAM constellation.

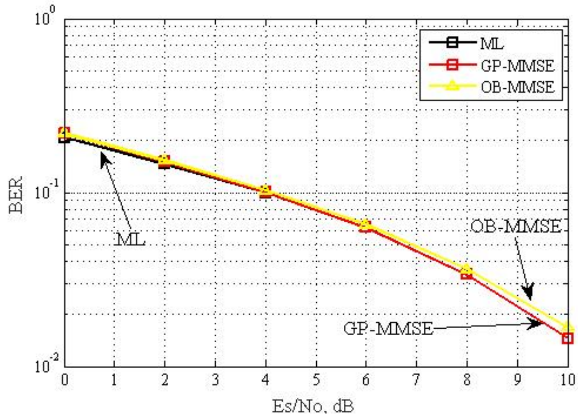


Fig. 9. Comparison of BER performance of ML, OB-MMSE, and GP-MMSE algorithms with $N_t = 8$, $N_r = 12$, $N_p = 3$ for 16PSK constellation.

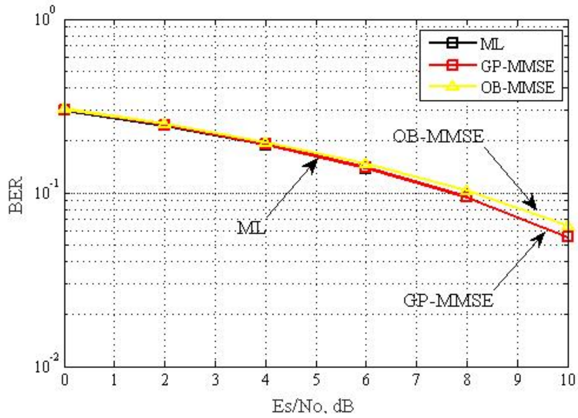


Fig. 10. Comparison of BER performance of ML, OB-MMSE, and GP-MMSE algorithms with $N_t = 6$, $N_r = 10$, $N_p = 3$ for 16PSK constellation.

Figure 10 provides a simulation when the number of activated antennas is increased to 3, with the condition of $N_t = 6$, $N_r = 10$, $N_p = 3$, $M = 16$. The simulation results indicate that the performance trends are similar to those observed when the number of activated antennas are 2, suggesting that increasing the number of activated antennas does not significantly alter the overall performance. The GP-MMSE algorithm still shows a better BER performance compared to OB-MMSE, demonstrating its robustness and efficiency even in scenarios with a higher number of activated transmit antennas.

Based on the above simulation results, we can conclude that the BER performance of the proposed algorithm under M-PSK constellation modulation is superior to that achieved under M-QAM constellation modulation. Specifically, the BER of the GP-MMSE algorithm under M-PSK modulation is very close to, and almost consistent with, the performance of the ML algorithm. In contrast, the OB-MMSE algorithm exhibits slightly inferior performance.

### *C. Computational Complexity Analysis*

To analyze the computational complexity of the GP-MMSE algorithm, we compare it directly with the computational complexities of ML and OB-MMSE algorithms. Given that the computation time for real number addition and subtraction is significantly lower than that for real number multiplication and division, we focus solely on the number of real number multiplication and division operations in our complexity analysis. $N_c = 2^{\left\lfloor \log_2 C_{N_t}^{N_p} \right\rfloor}$ represents the number of all possible transmit antenna combinations in the GSM system, $p_{avg}$ represents the average number of MMSE detections for each transmit antenna combinations in Eq. (12), and $L_j$ represents the number of adjacent constellation points with the minimum distance between the constellation symbol $\boldsymbol{s}_{\hat{j}}$ corresponding to the $j$-th activated antenna in the GP-MMSE algorithm. When the symbol is M-PSK modulation, $L_j = 3$ and $M$ is the modulation order.

The computational complexity of the ML algorithm can be obtained by utilizing Eq. (5), where the total number of all possible transmit antenna combinations is denoted as $N_c = 2^{\left\lfloor \log_2 C_{N_t}^{N_p} \right\rfloor}$, $2^{N_p \log_2 M}$ denotes the number of combinations where each antenna combination transmit different symbols, and for each combination $N_r N_p + N_r$ operations are required.

Therefore, the computational complexity of the ML algorithm can be expressed as

$$C_{\text{ML}} = 2^{N_p \log_2 M} N_r (N_p + 1) N_c \tag{22}$$

The computational complexity of the OB-MMSE detection algorithm, as reported in [11], can be expressed as:

$$\begin{aligned} C_{\text{OB-MMSE}} &= 2N_r N_t + N_c N_p \\ &+ N_c \left[ (2N_p^{\,3} + 3N_p^{\,2} - 5N_p) \big/ 6 + \left(N_p + 1\right)^2 N_r \right] p_{avg} \end{aligned} \tag{23}$$

where the first part $2N_r N_t$ represents the computational complexity associated with processing the received signal vector $\boldsymbol{y}$, i.e., specifically obtaining $\boldsymbol{z}$. The second part $N_c N_p$ is the computational complexity involved in calculating the weight value for each group of transmit antenna combinations; and the last part $N_c \left[ (2N_p^{\,3} + 3N_p^{\,2} - 5N_p) \big/ 6 + \left(N_p + 1\right)^2 N_r \right] p_{avg}$ represents the computational complexity required to detect the MMSE for all the antenna combinations sequentially and compute the total number of computations required to determine whether the current combination satisfies the judgment threshold value. Calculating $\boldsymbol{H}^{\text{H}}\boldsymbol{H}$ requires $(2N_p^{\,3} + 3N_p^{\,2} - 5N_p)/6$ operations [22], multiplying it with the matrix $\boldsymbol{H}^H$ requires $N_p^{\,2} N_r$ operations, and multiplying it with the matrix $\boldsymbol{y}$ requires $N_p N_r$ multiplication operations.

The GP-MMSE algorithm differs from the OB-MMSE algorithm in that its first part involves processing all received signals without the need to compute weight values. The computational complexity of this part is denoted as $N_c[(2N_p^{\,3} + 3N_p^{\,2} - 5N_p) \big/ 6 + \left(N_p + 1\right)^2 N_r] p_{avg} + 2N_r N_t$. The computational complexity of the GP-MMSE algorithm increases because it necessitates the application of a partial ML algorithm for the re-detection of modulated symbols and their adjacent constellation points. For M-QAM modulation, $MN_p$ operations are required to identify the set of adjacent constellation points with the minimum Euclidean distance from the given modulation symbol, and then $N_r \prod_{j=1}^{N_p} L_j (N_p + 1)$ operations are needed to perform ML detection on this current set of constellation points. For M-PSK modulation, since there are only two fixed adjacent constellation points that are closest to each modulation symbol, ML detection needs to be performed on the current set of three constellation points, requiring $3^{N_p}(N_p + 1) N_r$ operations.

The computational complexity of the GP-MMSE algorithm under M-QAM modulation and M-PSK modulation is shown in Eqs. (24)-(25), respectively.

$$\begin{aligned} C_{\text{M-QAM}} &= N_c \left[ (2N_p^{\,3} + 3N_p^{\,2} - 5N_p) \big/ 6 + \left(N_p + 1\right)^2 N_r \right] p_{avg} \\ &+ N_r \left[ 2N_t + \prod_{j=1}^{N_p} L_j (N_p + 1) \right] + MN_p \end{aligned} \tag{24}$$

$$\begin{aligned} C_{\text{M-PSK}} &= N_c \left[ (2N_p^{\,3} + 3N_p^{\,2} - 5N_p) \big/ 6 + \left(N_p + 1\right)^2 N_r \right] p_{avg} \\ &+ N_r \left[ 2N_t + 3^{N_p} (N_p + 1) \right] \end{aligned} \tag{25}$$

Figure 11 represents a comparison of the computational complexity of the ML, OB-MMSE and GP-MMSE algorithms when employing 16QAM modulation for $N_t = 8$, $N_r = 12$, $N_p = 2$. The horizontal axis represents the SNR and the vertical axis represents the computational complexity. As shown in Figure 11, the complexity of the ML algorithm is significantly higher than that of OB-MMSE and GP-MMSE algorithms. Furthermore, as the SNR increases, the complexity of both the GP-MMSE and OB-MMSE algorithms gradually decreases. At an SNR of 10dB, the ML algorithm exhibits a complexity of 147,456, whereas the

OB-MMSE algorithm has a complexity of approximately 1,132. The GP-MMSE algorithm, with a complexity of 1,740, lies slightly above the OB-MMSE algorithm in terms of complexity, but is significantly lower than the ML algorithm.

Figure 12 presents a comparison of the computational complexity of the ML, OB-MMSE, and GP-MMSE algorithms when using 64PSK modulation at $N_t = 6$, $N_r = 10$, $N_p = 3$. As the modulation order $M$ increases, it becomes evident that the computational complexity of the ML algorithm is significantly higher than that of the GP-MMSE algorithm. Meanwhile, although the computational complexity of the GP-MMSE algorithm gradually increases with increasing SNR, this increase is negligible when compared to the computational complexity of the GP-MMSE algorithm. Specially, at an SNR of 10dB, the ML algorithm exhibits a computational complexity of 786,432, whereas the GP-MMSE algorithm has a complexity of only 2,291, which is markedly lower.

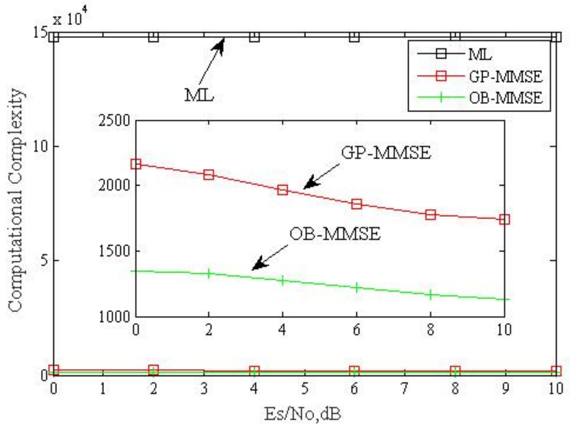


Fig. 11. The computational complexity comparison of ML, OB-MMSE, and GP-MMSE algorithms with $N_t = 8$, $N_r = 12$, $N_p = 2$ for 16QAM constellation.

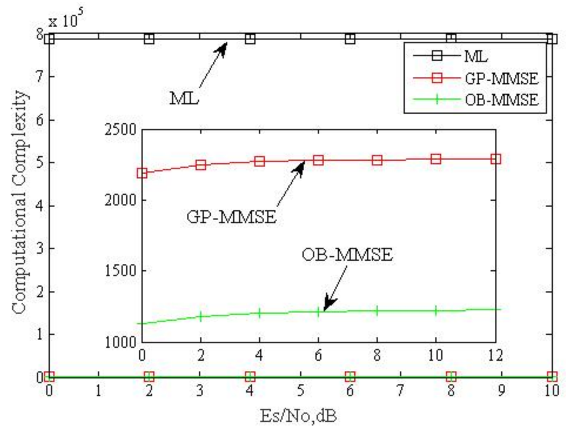


Fig. 12. The computational complexity comparison of ML, OB-MMSE, and GP-MMSE algorithms with $N_t = 6$, $N_r = 10$, $N_p = 3$ for 64PSK constellation.

## V. Conclusion

In this paper, a GP-MMSE detection algorithm based on group strategy specifically tailored for GSM system is proposed. Firstly, after selecting the antenna groups, the combinations of these antennas are reordered based on the sorting result obtained by a specific sorting algorithm for each antenna sequence. Subsequently, MMSE equalization processing and detection are sequentially applied to the sorted antenna combinations. Following this, the resulting modulation symbols are further optimized by incorporating a partial ML algorithm, which enhances the accuracy of modulation symbol estimation. Ultimately, the ML algorithm is employed to estimate the optimal transmit antenna combinations and symbols. Simulation results demonstrate that the performance of GP-MMSE algorithm is comparable to that of the ML algorithm and significantly outperforms the OB-MMSE algorithm. In particular, under M-PSK modulation, while the performance of GP-MMSE algorithm remains almost identical to that of the ML algorithm, its computational complexity is considerably lower.

## References


[1] R. Mesleh, H. Haas, C. W. Ahn, S. Yun, "Spatial modulation-A new low complexity spectral efficiency enhancing technique," in *Proc. IEEE International Conference on Communications and Networking in China,* Beijing, 2006, pp. 1-5.

[2] R. Mesleh, H. Haas, S. Sinanovic, W. Chang, S. Yun, "Spatial modulation," *IEEE Transactions on Vehicular Technology*, vol. 57, no. 4, pp. 2228-2241, 2008.

[3] M. Renzo, H. Haas, P. Grant, "Spatial modulation for multiple antenna wireless systems: A survey," *IEEE Communications Magazine*, vol. 49, no. 12, pp. 182-191, 2011.

[4] J. Jeganathan, A. Ghrayeb, L. Szczecinski, A. Ceron, "Space shift keying modulation for MIMO channels," *IEEE Transactions on Wireless Communications*, vol. 8, no. 7, pp. 3692-3703, 2009.

[5] X. Wang, "Research and analysis of large-scale MIMO channel modeling and spatial correlation," Master dissertation, Nanjing University of Information Science and Technology, Nanjing, 2022.

[6] C. Wang, F. Haider, X. Gao, X. You, Y. Yang, D. Yuan, "Cellular architecture and key technologies for 5G wireless communication networks, " *IEEE Communications Magazine*, vol. 52, no. 2, pp. 122-130, 2014.

[7] J. Fu, C. Hou, W. Xiang, L. Yan, Y. Hou, "Generalised spatial modulation with multiple active transmit antennas," in *Proc. 2010 IEEE Globecom Workshops*, Florida, 2010, pp. 839-844.

[8] A. Younis, N. Serafimovski, R. Mesleh, "Generalised spatial modulation," in *Proc. 2010 Conference Record of Forty Fourth Asilomar Conference on Signals*, Pacific Grove, California, 2010, pp. 1498-1502.

[9] J. Wang, S. Jia, J. Song, "Generalised spatial modulation system with multiple active transmit antennas and low complexity detection scheme," *IEEE Transactions on Wireless Communications*, vol. 11, no. 4, pp. 1605-1615, 2012.

[10] R. Legnain, R. Hafez, I. Marsl, "A novel spatial modulation using MIMO spatial multiplexing," in *Proc. 2013 1st International Conference on Communications, Signal Processing, and their Applications (ICCSPA)*, Sharjah, United Arab Emirates, 2013, pp. 1-4.

[11] Y. Xiao, Z. Yang, L. Dan, "Low-complexity signal detection for generalized spatial modulation," *IEEE Communications Letters*, vol. 18, no. 3, pp. 403-406, 2014.

[12] J. Cal-Braz, C. Medina, R. Sampaio-Neto, "Group maximum likelihood detection in generalized spatial modulation," in *Proc. The Tenth International Symposium on Wireless Communication Systems*, Ilmenau, Germany, 2013, pp. 1-4.

[13] J. Cal-Braz, R. Sampaio-Neto, "Nested maximum likelihood group detection in generalized spatial modulation MIMO systems," *IEEE Communications Letters*, vol. 18, no. 6, pp. 953-956, 2014.

[14] F. Chen, F. Change, "Low-complexity signal detection algorithm for generalized spatial modulation," *Application Research of Computers*, vol. 34, no. 3, pp. 846-848, 2017.

[15] J. Cal-Braz, R. Sampaio-Neto, "Projection-based list detection in generalized spatial modulation MIMO systems," *IEEE Communications Letters*, vol. 19, no. 7, pp. 1145-1148, 2015.

[16] M. Elsayed, H. Hussein, U. Mohamed, "Fully generalized spatial modulation," in *Proc. 2018 35th National Radio Science Conference (NRSC)*, Cairo, Egypt, 2018, pp. 274-282.

[17] R. Rajashekar, K. Hari, L. Hanzo, "Reduced-complexity ML detection and capacity-optimized training for spatial modulation systems," *IEEE Transactions on Communications*, vol. 62, no. 1, pp. 112-125, 2014.

[18] H. Men, M. Jin, "Low-complexity optimal MPSK detection for spatial modulation," *Journal on Communications*, vol. 36, no. 8, pp. 118-124, 2015.
[19] X. Zhang, S. Zhang, "Low-complexity GSM detection based on iterative zero forcing and minimum mean square error," *Engineering Letters*, vol. 32, no. 3, pp. 677-683, 2024.
[20] X. Zhang, H. Tan, W. Lv, "A low-complexity detection algorithm for generalized space shift keying systems," *IAENG International Journal of Computer Science*, vol. 49, no. 2, pp. 364-368, 2022.
[21] G. Duan, "Research on antenna selection and detection algorithm in generalized spatial modulation system," Master dissertation, Chang'an University, Xi'an, 2019.
[22] R. Farebrother. Linear least squares computations. New York: Marcel Dekker, Inc., 1988, pp. 77-92.

**Xinhe Zhang** was born in Hebei Province, P. R. China, received the B.S. degree in Application of Electronic Technology from Anshan Iron and Steel Technology, Anshan, P. R. China, the M.S. degree in Control Theory and Control Engineering from Anshan University of Science and Technology, Anshan, P. R. China, the Ph.D. degree in Communication and Information Systems from Dalian University of Technology, Dalian, P. R. China, in 2002, 2005, 2017. His research interests include signal processing and compressed sensing.

**Siyu Zhang** received the B. S. degree in Electronic and Information Engineering from Nantong University, Nantong, P. R. China in 2020. She has received the M. S. degree in University of Science and Technology Liaoning, Anshan, P. R. China. Her main research interests are signal detection and wireless communication.